Lipids in Health and Disease

RESEARCH

Open Access

Dihydromyricetin suppresses endothelial NLRP3 inflammasome activation and attenuates atherogenesis by promoting mitophagy

Qin Hu[1], Chengying Li[1], Ting Zhang[2], Long Yi[2], Yifan Shan[1], Xiangyu Ma[1], Tongjian Cai[1], Li Ran[2], Hui Shen[2] and Yafei Li[1*]

Abstract

Background NOD-like receptor protein 3 (NLRP3) inflammasome activation is indispensable for atherogenesis. Mitophagy has emerged as a potential strategy to counteract NLRP3 inflammasome activation triggered by impaired mitochondria. Our previous research has indicated that dihydromyricetin, a natural flavonoid, can mitigate NLRP3-mediated endothelial inflammation, suggesting its potential to treat atherosclerosis. However, the precise underlying mechanisms remain elusive. This study sought to investigate whether dihydromyricetin modulates endothelial mitophagy and inhibits NLRP3 inflammasome activation to alleviate atherogenesis, along with the specific mechanisms involved.

Methods Apolipoprotein E-deficient mice on a high-fat diet were administered daily oral gavages of dihydromyricetin for 14 weeks. Blood samples were procured to determine the serum lipid profiles and quantify proinflammatory cytokine concentrations. Aortas were harvested to evaluate atherosclerotic plaque formation and NLRP3 inflammasome activation. Concurrently, in human umbilical vein endothelial cells, Western blotting, flow cytometry, and quantitative real-time PCR were employed to elucidate the mechanistic role of mitophagy in the modulation of NLRP3 inflammasome activation by dihydromyricetin.

Results Dihydromyricetin administration significantly attenuated NLRP3 inflammasome activation and vascular inflammation in mice on a high-fat diet, thereby exerting a pronounced inhibitory effect on atherogenesis. Both in vivo and in vitro, dihydromyricetin treatment markedly enhanced mitophagy. This enhancement in mitophagy ameliorated the mitochondrial damage instigated by saturated fatty acids, thereby inhibiting the activation and nuclear translocation of NF-κB. Consequently, concomitant reductions in the transcript levels of NLRP3 and interleukin-1β (IL-1β), alongside decreased activation of NLRP3 inflammasome and IL-1β secretion, were discerned. Notably, the inhibitory effects of dihydromyricetin on the activation of NF-κB and subsequently the NLRP3 inflammasome were determined to be, at least in part, contingent upon its capacity to promote mitophagy.

*Correspondence:
Yafei Li
liyafei2008@hotmail.com

Full list of author information is available at the end of the article

Conclusion This study suggested that dihydromyricetin may function as a modulator to promote mitophagy, which in turn mitigates NF-κB activity and subsequent NLRP3 inflammasome activation, thereby conferring protection against atherosclerosis.

Keywords Atherosclerosis, Dihydromyricetin, Mitophagy, NLRP3 inflammasome, Vascular endothelium

Introduction

Vascular endothelial dysfunction, which leads to persistent and chronic vascular inflammation, is the pathological foundation of atherosclerosis [1]. Activation of the endothelial NOD-like receptor protein 3 (NLRP3) inflammasome directly leads to endothelial dysfunction during hypercholesterolemia [2]. Similarly, our previous study revealed that palmitic acid (PA), the most abundant saturated fatty acid in human blood, significantly induces NLRP3-mediated pyroptosis and the secretion of the proinflammatory cytokine interleukin-1β (IL-1β) in vascular endothelial cells [3]. Moreover, recent studies have yielded substantial evidence underscoring the pivotal role of the NLRP3 inflammasome in the inflammatory process associated with atherosclerosis. Consequently, the inhibition of endothelial NLRP3 inflammasome activation holds exceptional importance for the prevention and treatment of atherosclerosis.

The NLRP3 inflammasome is activated by the convergence of two signals [4]. The priming signal (signal 1) depends on the transcription factor nuclear factor kappa-B (NF-κB), which controls the transcription of NLRP3 and the proinflammatory cytokine IL-1β [5]. The activation signal (signal 2) encompasses the intracellular recruitment and assembly of the NLRP3 inflammasome, culminating in the caspase1-dependent release of the pro-inflammatory cytokines IL-1β and IL-18, as well as in the gasdermin D-mediated pyroptosis [6]. Studies have substantiated that mitochondrial dysfunction is indispensable for the activation of NLRP3 inflammasome [5, 7, 8]. However, the precise signal—whether signal 1 or signal 2—that mitochondrial damage induces to activate the NLRP3 inflammasome remains enigmatic. Notwithstanding, it is imperative to underscore that mitigating mitochondrial dysfunction or selectively eliminating damaged mitochondria may constitute efficacious strategies to impede NLRP3 inflammasome activation, thereby preserving normal mitochondrial functionality. The autophagic clearance of impaired mitochondria, a process known as mitophagy, epitomizes one of the most prevalent mechanisms through which cells sustain a healthy mitochondrial pool [9]. Consequently, augmenting mitophagy could emerge as an effective stratagem for inhibiting endothelial NLRP3 inflammasome activation.

Dihydromyricetin (DHM) is a natural flavonoid phytochemical predominantly found in various plant species, such as *Ampelopsis grossedentata* and *Hovenia dulcis*. The abundance of DHM is particularly notable in the stems and leaves of *Ampelopsis grossedentata*, where the DHM content exceeds 20% (by dry weight). DHM exhibits multifaceted pharmacological activities, encompassing antioxidant, anti-inflammatory, and lipid-lowering effects. Previous research has indicated that DHM ameliorates NLRP3 inflammasome-dependent inflammatory injury in the endothelium, alleviates hyperlipidaemia, and forestalls aortic inflammation, thereby suggesting its potential for treating atherosclerosis [3, 10]. However, the molecular mechanisms through which DHM influences endothelial function, vascular inflammation, and atherosclerosis remain largely unexplored. Studies have intimated that DHM efficaciously upregulates MAP1LC3/LC3 (LC3) expression and promotes autophagosome formation [11, 12], which may underpin the promotion of mitophagy. Nevertheless, it remains elusive whether DHM modulates endothelial mitophagy and thereby impedes NLRP3 inflammasome activation, along with the specific mechanisms involved.

Hence, this study delved into the role and underlying mechanisms of DHM in the modulation of endothelial NLRP3 inflammasome during atherogenesis, employing both in vivo and in vitro models. This study endeavored to furnish a robust experimental underpinning for the potential application of DHM as a preventive and therapeutic adjuvant for atherosclerosis and other diseases characterized by abnormal NLRP3 expression.

Materials and methods

Reagents

Human umbilical vein endothelial cells (HUVECs, PUMC-HUVEC-T1) were obtained from the American Type Culture Collection (ATCC). Endothelial cell medium (ECM; 1001) and endothelial cell growth supplement (ECGS, 1052) were obtained from ScienCell Research Laboratories (San Diego, CA, USA). Foetal bovine serum (FBS; 04-001-1ACS) was obtained from Biologic Industries (Kibbutz Beit Haemek, Israel). Trypsin-EDTA (0.25%) (25200-056) was obtained from Gibco (Grand Island, NY, USA). DHM (A0049tqw50g) was obtained from Chengdu MUST Bio-Technology Co., Ltd. (Sichuan, China). DHM (42866) and palmitic acid (P0500) for cell culture, dimethyl sulfoxide (DMSO, D2650), carbonyl cyanide m-chlorophenyl hydrazone (CCCP, C2759), chloroquine (CQ, C6628), anti-LC3B (L7543, 1:1000), and an anti-β-actin antibody (A5441, 1:1000) were obtained from Sigma Aldrich (St. Louis, MO, USA). Antibodies against NF-κB p65 (sc-8008,

1:500), sequestosome 1 (SQSTM1/p62, sc-28359, 1:500), TIM23 (sc-514463, 1:500), and Parkin (sc-32282, 1:500) were obtained from Santa Cruz Biotechnology (Santa Cruz, CA, USA). Mitochondrial division inhibitor 1 (Mdivi-1, HY-15886) was obtained from MedChem Express (Greenville, USA). An anti-NLRP3 antibody (NBP2-12446, 1:500) was purchased from Novus Biologicals (Littleton, CO, USA). Antibodies against caspase-1 (3866s, 1:1000), phospho-NF-κB p65 (p-p65, 3033s, 1:1000), IL-1β (12703, 1:1000), and MitoTracker® Deep Red FM (MTDR, 8778) were obtained from Cell Signaling Technology (Beverly, MA, USA). A cell counting kit-*8* (CCK-8; CK04) was obtained from Dojindo Laboratories (Kyushu, Japan). An anti-PINK1 antibody (GB114934) and human IL-1β (GEH0002), TNF-α (GEH0004), and IL-6 (GEH0001) enzyme-linked immunosorbent assay (ELISA) kits were obtained from Servicebio Technology Co., Ltd. (Wuhan, China). Mouse IL-1β (GEM0002), IL-18 (GEM0010), TNF-α (GEM0004), and IL-6 (GEM0001) ELISA kits were obtained from Servicebio Technology Co., Ltd. (Wuhan, China). NF-κB activation, a nuclear translocation assay kit (SN368), and a mitochondrial membrane potential assay kit with JC-1 (C2006) were obtained from Beyotime Biotechnology (Jiangsu, China). A mouse NLRP3 ELISA kit (ml037234) was obtained from Shanghai Enzyme-linked Biotechnology Co., Ltd. (Shanghai, China). A mouse caspase-1 ELISA kit (D721050) was obtained from Sangon Biotech (Shanghai) Co., Ltd. (Shanghai, China).

Mice and interventions

Referring to previous studies [13–15], this study utilized apolipoprotein E-deficient ($ApoE^{-/-}$, C57BL/6J background) mice maintained on a high-fat diet (HFD) to establish a murine model of atherosclerosis. Six-week-old male $ApoE^{-/-}$ mice were purchased from Cavens Lab Animal Co. (Changzhou, China) and maintained under SPF conditions at the Experimental Animal Center of the Third Military Medical University (Chongqing, China) under a 12-hour light/dark cycle. Following a two-week adaptation period, the mice were randomly allocated into four distinct groups: (i) the control group; (ii) the HFD group; (iii) the HFD+50 mg/kg DHM group; and (iv) the HFD+200 mg/kg DHM group. Mice in the control group were fed a normal diet, and those in the remaining three groups were fed a high-fat diet (containing 40 kcal% fat and 1.25% cholesterol, Supplementary Table 1) for 14 weeks. Throughout the study, the mice in the control and HFD groups received placebo, whereas those in the HFD+50 mg/kg DHM and HFD+200 mg/kg DHM groups received DHM (50 mg/kg body weight or 200 mg/kg body weight) via oral gavage every day for 14 weeks. The doses of DHM utilized in this study were determined based on previous reports documenting its beneficial pharmacological impacts on animals with diverse diseases [10, 16–18]. Throughout the 14-week study period, food consumption and body weight were monitored weekly. After 14 weeks of intragastric administration, the mice were fasted overnight and then euthanized under pentobarbital sodium anaesthesia (50 mg/kg body weight). Blood, the aortic root, and the whole aorta (including the aortic arch and thoracic and abdominal regions) were collected as previously described [19, 20]. All experiments involving animals were conducted in full compliance with the National Institutes of Health Guide for the Care and Use of Laboratory Animals and were authorized by the Laboratory Animal Welfare and Ethics Committee of the Third Military Medical University (Chongqing, China) (number: AMUWEC2020068).

Serum lipid profile measurements

Blood samples were collected to determine the concentrations of serum triglycerides (TG, S03027), total cholesterol (TC, S03042), low-density lipoprotein cholesterol (LDL-C, S03029), and high-density lipoprotein cholesterol (HDL-C, S03025) using kits from Rayto Life and Analytical Sciences Co., Ltd. (Guangdong, China), with protocols provided by the manufacturer.

Inflammatory factor analysis

The serum concentrations of proinflammatory cytokines such as IL-1β, IL-18, TNF-α, and IL-6, as well as the levels of NLRP3 and caspase-1, were quantified via ELISA following the manufacturer's recommended procedures.

Atherosclerotic lesion analysis

The en face aorta, including the aortic arch and thoracic and abdominal regions, as well as the cross-sectional aortic sinus, were analysed using Oil Red O staining to quantify atherosclerotic lesions, following previously described methods [14, 20]. The whole aorta, from the aortic root to the common iliac artery bifurcation, was isolated and dissected, and all connective tissues were removed and then sectioned longitudinally. After staining with Oil Red O, digital images of the en face aortas were captured, and the atherosclerotic lesions were quantified as a percentage of the total surface area using ImageJ imaging software (Bethesda, MD, USA). For the analysis of atherosclerotic lesions in the aortic sinus, the aortic sinuses were embedded in OCT compound (Sakura, Chiba, Japan) and frozen at -20 °C. Sections with a thickness of 10 μm were then collected, starting from the aortic root and extending 400 μm, as detailed in previous studies [21]. Every tenth section was stained with Oil Red O and haematoxylin for visualization, after which the lesion areas were quantitatively analysed using ImageJ imaging software (Bethesda, MD, USA).

Immunohistochemistry

Aortic vessel sections were subjected to staining with primary antibodies against Parkin (Servicebio, Wuhan, China, 1:200) at 4 °C overnight. Subsequently, secondary antibodies were applied. Thereafter, the sections were stained with diaminobenzidine. Ultimately, images of the tissues were captured using a fluorescence microscope.

Cell culture and treatment

HUVECs were cultured in ECM supplemented with 5% FBS, 1% ECGS, 100 μg/mL streptomycin, and 100 U/mL penicillin. The culture was maintained in a CO_2 incubator at 37 °C with 5% CO_2 and 100% relative humidity. When the cells reached 80-90% confluence, adherent HUVECs were isolated using trypsin-EDTA treatment and either passaged or used for subsequent experiments. To model endothelial injury, HUVECs were pretreated with PA for 24 h, as previously described [3]. In addition, to examine the effect of DHM on mitophagy in vascular endothelial cells, HUVECs were treated with different concentrations of DHM (0.1, 1, or 10 μmol/L) for 12 h and then treated with PA for another 24 h. The doses of DHM utilized in this study were based on our previous study [3]. Alternatively, for mitophagy manipulation experiments, HUVECs were pretreated with either CCCP (10 μmol/L) or Mdivi-1 (20 μmol/L) for 1 h prior to DHM treatment to induce or inhibit mitophagy, respectively.

Cell viability assays

HUVECs in the logarithmic growth phase were seeded into a 96-well plate (Corning, NY, USA) at a density of 5,000 cells per well in complete medium and then incubated overnight for cell attachment before further treatment. Following treatment of the cells according to the respective protocols, 10 μL of a solution from the Cell Counting Kit-8 (CCK-8) was added to each well, and the plates were incubated for an additional 1 to 2 h. Thereafter, the optical density at a wavelength of 450 nm was measured using a microplate spectrophotometer (Thermo, MA, USA).

Detection of the mitochondrial membrane potential (ΔΨm)

HUVECs in the logarithmic growth phase were seeded into a 12-well microplate (Corning, USA), with three replicate wells for each treatment condition. After exposing the HUVECs to the designated treatments, the alterations in the mitochondrial membrane potential were assessed with a JC-1 mitochondrial membrane potential detection kit (Beyotime, Shanghai, China). The analyses were performed using a multifunctional microplate reader or a fluorescence microscope following protocols described in the literature [22, 23]. JC-1 fluorescence intensity was measured at excitation/emission (Ex/Em) wavelengths of 514/529 nm for green fluorescence (JC-1 monomers) and 585/590 nm for red fluorescence (JC-1 aggregates). Mitochondrial depolarization was defined as a decrease in the ratio of red to green fluorescence.

Mitophagy determination by flow cytometry

Mitophagy was evaluated via a flow cytometry-based approach, as previously described [24, 25], employing MTDR, a widely used mitochondria-selective probe. Briefly, adherent HUVECs were dissociated using trypsin and resuspended in complete medium containing 10 nM MTDR. The plates were subsequently incubated for 20 min at 37 °C. Following two washes with PBS, the cells were resuspended in cold PBS for flow cytometry analysis using a BD Accuri™ C6 Plus flow cytometer (BD Biosciences Systems, CA, USA). The resulting data were analysed using FlowJo software (ver. 10.5.3, BD Biosciences Systems, CA, USA). The mean fluorescence intensity in the FL4 channel, corresponding to the viable cell population, was plotted and normalized to the mean fluorescence intensity of the control group.

ELISA of inflammatory factors in culture supernatant

Upon completion of the assigned treatments, the culture supernatants were retrieved and centrifuged to eliminate any sedimentation. Thereafter, the concentrations of proinflammatory cytokines such as IL-1β, IL-6, and TNF-α were quantified using ELISA kits (Servicebio, Wuhan, China) in accordance with the manufacturer's instructions.

NF-κB activation and nuclear translocation assay

After the cells were subjected to the designated treatments, NF-κB activation and nuclear translocation assays were performed using an NF-κB activation and nuclear translocation assay kit (Beyotime, Shanghai, China) according to the manufacturer's protocols. Images were captured under a fluorescence microscope. NF-κB p65 was visualized by red fluorescence, while the DAPI-stained nuclei appeared blue.

Western blotting analysis

After the indicated treatments, the cells were detached and homogenized in RIPA lysis buffer (Beyotime, Shanghai, China) supplemented with PMSF solution (Beyotime, Shanghai, China). The total protein concentration was quantified using the BCA Protein Assay Kit (Beyotime, Shanghai, China) following the manufacturer's recommended procedures. Forty micrograms of total protein extracted per sample was then separated via sodium dodecyl sulfate-polyacrylamide gel electrophoresis (SDS–PAGE) and transferred onto polyvinylidene difluoride (PVDF) membranes using standard Western blotting techniques. The membranes were subsequently blocked with a 5% (wt/vol) solution of bovine

serum albumin in phosphate-buffered saline with 0.1% Tween 20 and then incubated with the designated primary antibodies. This was followed by the addition of the corresponding secondary antibodies. The blots were developed with a BeyoECL Plus kit (Beyotime, Shanghai, China) and visualized on an Odyssey imager (LI-COR Biosciences, USA). Densitometric analysis of the scanned images was performed using ImageJ software. β-actin (ABclonal, Wuhan, China) served as a loading control. The values are expressed as the fold change relative to the control group.

Quantitative real-time PCR

Cells or aortas from ApoE$^{-/-}$ mice that had been treated according to the designated protocol were lysed in TRIzol reagent (Invitrogen, CA, USA) to extract total RNA following the manufacturer's instructions. Reverse transcription was then performed to synthesize complementary DNA (cDNA) using reverse transcriptase (Servicebio, Wuhan, China). Subsequently, triplicate RT-PCR analyses were conducted using Universal Blue SYBR Green qPCR Master Mix (Servicebio, Wuhan, China). The mRNA expression levels in each sample were normalized to the GAPDH expression level and are expressed as the fold change relative to the control using the comparative Ct (ΔΔCT) method. The gene-specific sequences of the primers used are listed in Table 1.

Statistical analysis

The data are presented as the mean ± standard deviation (SD), and the experiments were repeated at least three times. For between-group comparisons, one-way analysis of variance (ANOVA) followed by Bonferroni's multiple comparison test was employed. All statistical analyses were carried out using SPSS statistical software (version 26.0, IBM). A P value < 0.05 was considered to indicate statistical significance.

Results

DHM protects against HFD-induced atherosclerosis in vivo

Previous research has demonstrated that DHM can mitigate endothelial inflammatory injury and ameliorate hyperlipidaemia, suggesting that DHM is a potential therapeutic adjuvant for treating atherosclerosis [3, 17]. To test this hypothesis, we established an atherosclerosis mouse model in ApoE$^{-/-}$ mice fed a HFD and administered DHM via gastric perfusion. After 14 weeks of intragastric administration, the ApoE$^{-/-}$ mice were sacrificed under anaesthesia, and their blood and aortas were collected for analysis. Given that dyslipidaemia is one of the major risk factors for atherosclerosis, we first investigated the impact of DHM intervention on the serum levels of lipids in mice. Compared with those in the HFD group, the serum TC (Fig. 1A), TG (Fig. 1B), and LDL-C (Fig. 1C) levels were significantly lower in the DHM intervention group. Moreover, DHM treatment markedly increased the level of HDL-C (Fig. 1D). On this basis, we further explored the impact of DHM intervention on plaque formation. Grossly obvious atherosclerotic lesions were observed after staining the aortas with Oil Red O (Fig. 1E and G). As shown in Fig. 1, there were noticeably more plaques on the whole aorta or aortic roots in the HFD groups than in the control group. However, the administration of DHM (50 mg/kg bw and 200 mg/kg bw) significantly decreased the plaque area (Fig. 1E-H). Taken together, these findings suggest that DHM mitigates atherogenesis.

DHM impedes NLRP3 inflammasome activation and reduces vascular inflammation in vivo

Given the association between the NLRP3 inflammasome and atherosclerosis [26], as well as the mitigating effect of DHM treatment on NLRP3-mediated inflammation [3], we sought to investigate whether DHM intervention could inhibit NLRP3 inflammasome activation and attenuate vascular inflammation in vivo. As illustrated in Fig. 2, DHM significantly abrogated the upregulation of NLRP3 and caspase-1 expression under high-fat diet conditions, leading to decreases in the serum IL-1β, IL-18, IL-6, and TNF-α levels. Additionally, compared to those in the control group, the transcript levels of NLRP3 and IL-1β in the aorta were significantly greater in the HFD group, and these changes were notably attenuated by DHM administration (Fig. 2G and H). Taken together, these results demonstrate that DHM inhibits NLRP3 inflammasome activation and relieves vascular

Table 1 Primers used for real-time PCR

Gene	NCBI Reference Sequence	Primer sequence	
		Forwards	Reverse
Mouse NLRP3	NM_001359638.1	GCTAAGAAGGACCAGCCAGAGTG	TTACAAATGGAGATGCGGGAGA
Mouse IL-1β	NM_008361.4	AGGCTCCGAGATGAACAACAAA	GTGCCGTCTTTCATTACACAGGA
Mouse LC3	NM_001364358.1	CCGTCCGAGAAGACCTTCAA	TCTTGCGGCAGGAGAACCTA
Mouse GAPDH	NM_008084.2	CCTCGTCCCGTAGACAAAATG	TGAGGTCAATGAAGGGGTCGT
Human NLRP3	NM_001079821.2	ATTGAGCACCAGCCATTCCC	GAGTGTTGCCTCGCAGGTAAAG
Human IL-1β	NM_000576.2	CGATCACTGAACTGCACGCTC	ACAAAGGACATGGAGAACACCACTT
Human GAPDH	NM_002046	GGAAGCTTGTCATCAATGGAAATC	TGATGACCCTTTTGGCTCCC

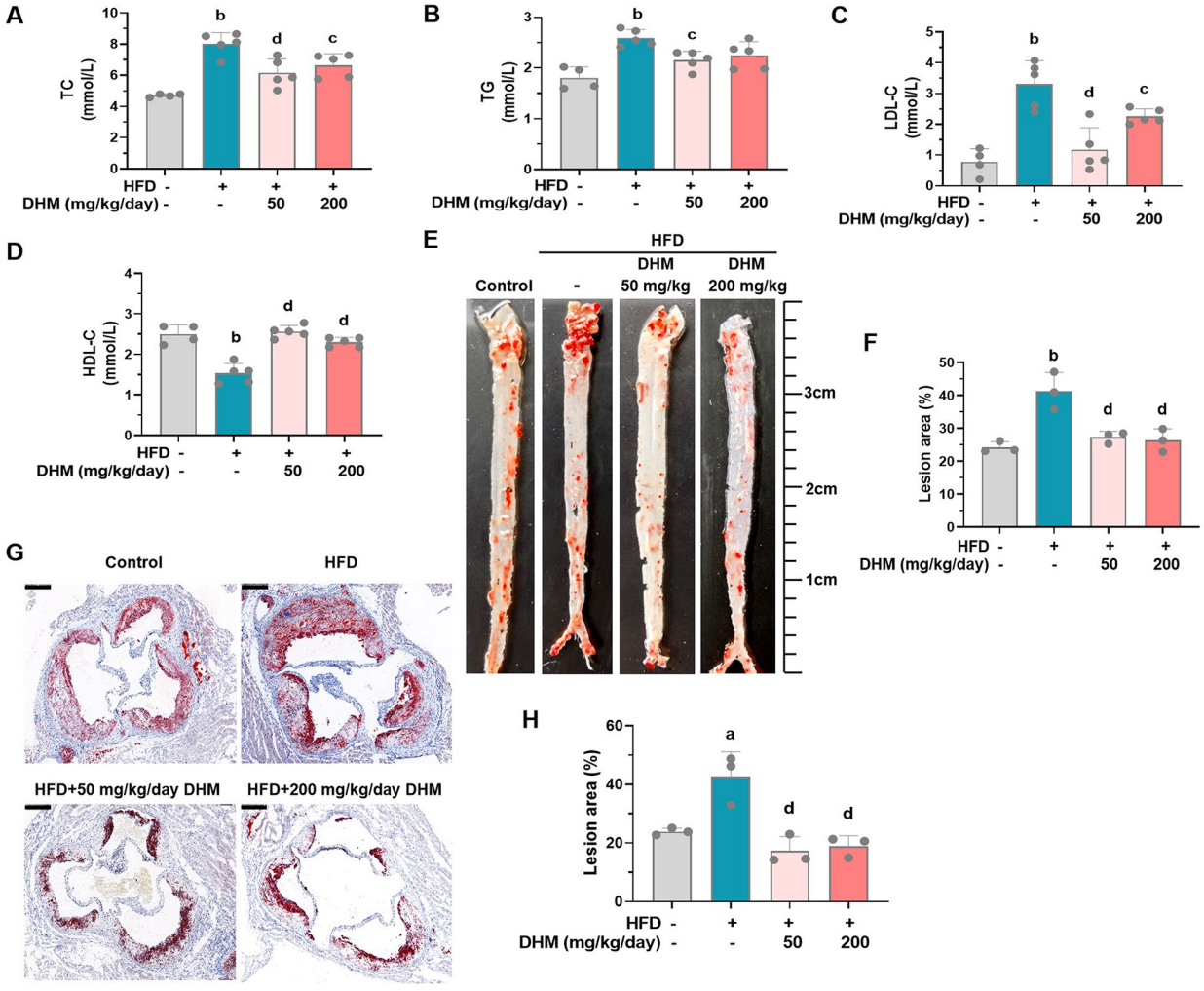

Fig. 1 DHM protects against HFD-induced atherosclerosis in vivo. The serum concentrations of TC (**A**), TG (**B**), LDL-C (**C**), and HDL-C (**D**) were measured ($n=5$). (**E**) Oil Red O staining was performed to visualize atherosclerotic lesions in the whole aorta. (**F**) The bars show the lesion area percentage. (**G**) Representative images of aortic sinus lesions stained with Oil Red O (counterstained with haematoxylin) were obtained. Scale bars = 200 μm. (**H**) The bars show the lesion area percentage. The values are expressed as the mean ± SD. $^{a}P<0.05$ or $^{b}P<0.01$ (versus the control group); $^{c}P<0.05$ or $^{d}P<0.01$ (versus the HFD group). DHM, dihydromyricetin; HDL-C, high-density lipoprotein cholesterol; HFD, high-fat diet; SD, standard deviation; LDL-C, low-density lipoprotein cholesterol; TC, total cholesterol; TG, triglycerides

inflammation, ultimately decelerating the progression of atherosclerosis.

DHM reduces NLRP3 expression and inflammasome activation in endothelial cells

Endothelial cell dysfunction is an important contributor to the pathophysiology of atherosclerosis and has a profound influence on the coordination of both acute and chronic inflammation within the arterial wall [27, 28]. Next, we investigated the specific mechanisms by which DHM hampers the activation of the NLRP3 inflammasome in endothelial cells. PA, the most abundant saturated fatty acid in blood, is commonly found in animal fat and can increase LDL-C levels in blood and induce inflammation and oxidative stress in endothelial cells, both of which are implicated in the pathogenesis of atherosclerosis. As expected, PA treatment notably increased the secretion of the endothelial inflammatory factors IL-1β, IL-6, and TNF-α (Fig. 3A-C). Moreover, PA significantly increased caspase-1 cleavage and IL-1β maturation (Fig. 3D-E), indicating that PA activated the NLRP3 inflammasome. In contrast, DHM pretreatment significantly inhibited caspase-1 cleavage and IL-1β maturation and secretion in PA-stimulated endothelial cells (Fig. 3F-H). These results indicate that DHM pretreatment suppresses NLRP3 inflammasome activation. Furthermore, considering the essential role of NLRP3 expression in the assembly and activation of the NLRP3 inflammasome, we investigated the effects of DHM on NLRP3 expression. DHM pretreatment markedly

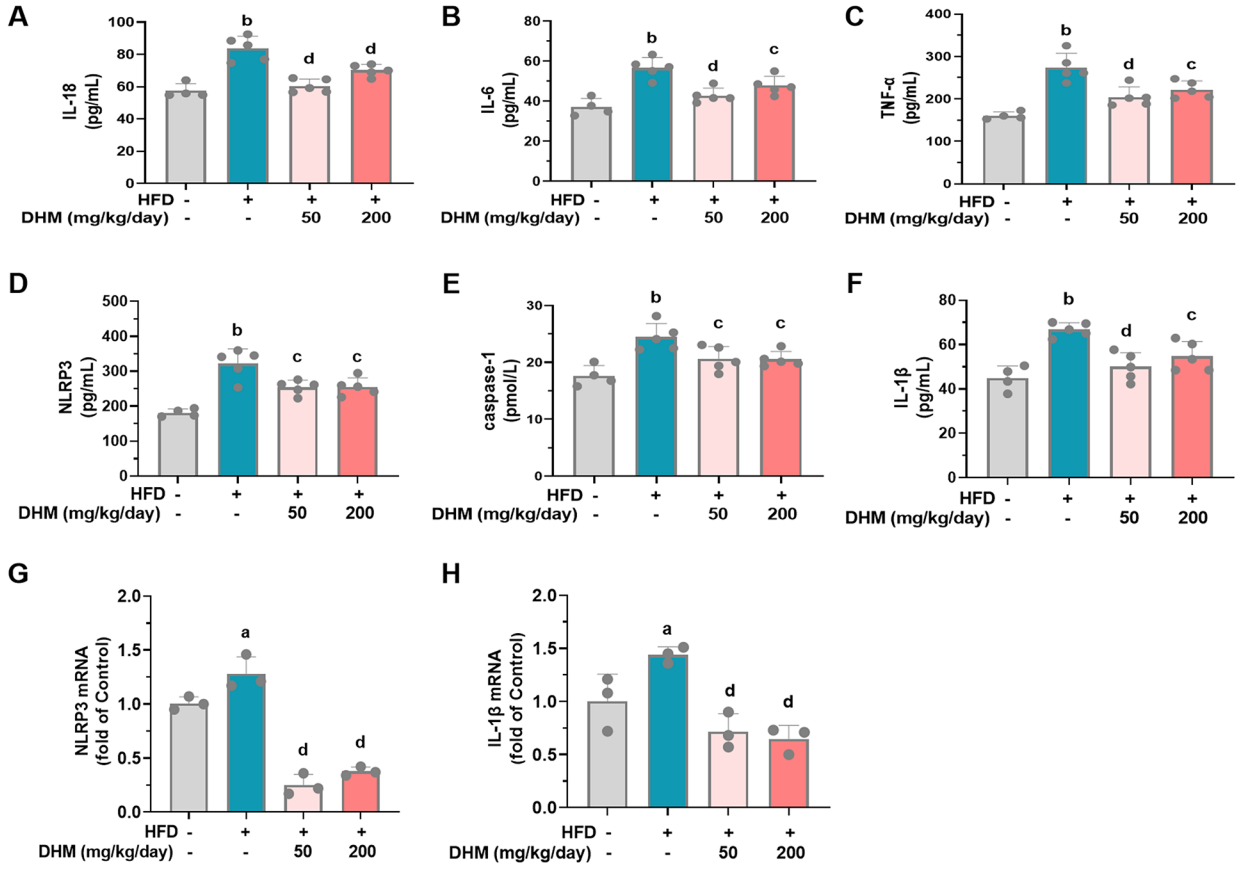

Fig. 2 DHM impedes NLRP3 inflammasome activation and reduces vascular inflammation in vivo. (**A**-**F**) Blood samples were centrifuged to separate the serum, which was subsequently subjected to ELISA to evaluate the levels of IL-18 (A), IL-6 (B), and TNF-α (**C**) and those of NLRP3 (**D**), caspase-1 (**E**), and IL-1β (**F**) ($n = 5$). (**G**-**H**) RT–PCR was performed to estimate the mRNA expression of NLRP3 (**G**) and IL-1β (**H**) in the aorta. The values are expressed as the mean ± SD. $^{a}P < 0.05$ or $^{b}P < 0.01$ (versus the control group); $^{c}P < 0.05$ or $^{d}P < 0.01$ (versus the HFD group). DHM, dihydromyricetin; ELISA, enzyme-linked immunosorbent assay; HFD, high-fat diet; IL-6, interleukin-6; IL-18, interleukin-18; IL-1β, interleukin-1β; NLRP3, NOD-like receptor protein 3; SD, standard deviation; TNFα, tumor necrosis factor α

inhibited NLRP3 protein expression (Fig. 3G-H). Additionally, NLRP3 mRNA expression was also notably decreased by DHM pretreatment (Fig. 6D). These data indicate that DHM blocks NLRP3 expression at both the protein and mRNA levels, thereby substantially inhibiting NLRP3 inflammasome activation.

DHM enhances endothelial mitophagy and mitigates mitochondrial damage

Given the close association between mitochondrial dysfunction and NLRP3 inflammasome activation [29, 30], this study further investigated the effects of DHM on mitochondrial function in response to PA stimulation. As shown in Fig. 4, these results revealed that PA-induced mitochondrial damage, as evidenced by a decrease in the mitochondrial membrane potential, was alleviated by DHM treatment (Fig. 4A-B). Mitophagy is a critical process for regulating mitochondrial number and maintaining normal mitochondrial function. Therefore, we proceeded to assess the effect of DHM on mitophagy in endothelial cells. Using a previously described flow cytometry-based methodology [24], this study revealed that DHM significantly increased the fluorescence intensity of MTDR in endothelial cells pretreated with CQ which inhibits lysosomal function (Fig. 4C). This finding suggested that DHM promotes mitophagy in these cells. Moreover, an elevated LC3II/I ratio and Parkin expression, along with decreased expression of the mitochondrial protein TIM23, serve as well-recognized mitophagy markers [31]. PCR and Western blot analyses revealed that DHM significantly increased the LC3-II/LC3-I ratio and PINK1 and Parkin expression in endothelial cells while decreasing p62 levels and the expression of the mitochondrial protein TIM23 (Fig. 4D and F). Concurrently, DHM markedly elevated Parkin and PINK1 expression, as well as LC3 mRNA and protein levels, in mouse aortas (Fig. 4G and J). These findings confirm that DHM promotes mitophagy both in vitro and in vivo.

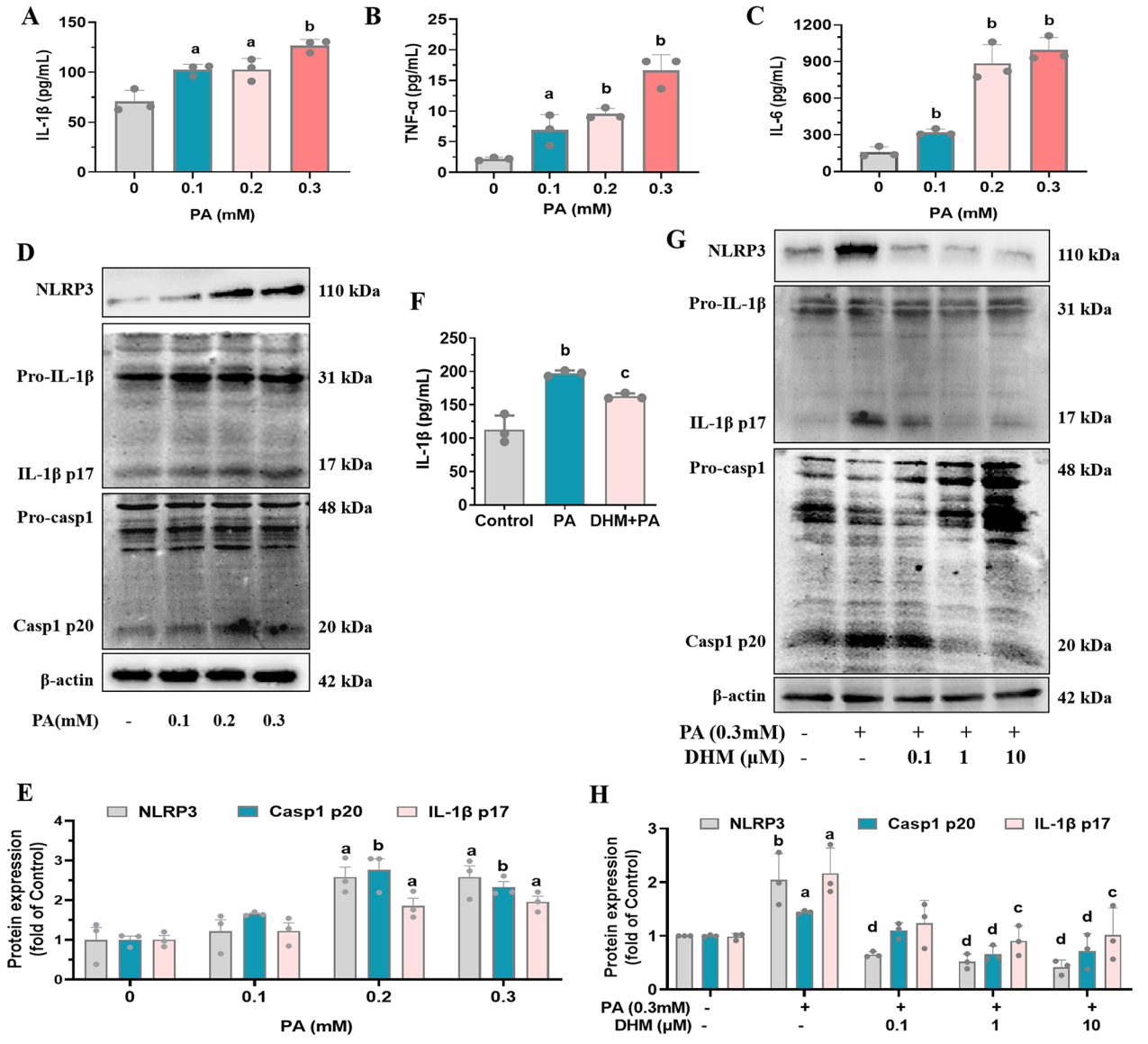

Fig. 3 DHM reduces NLRP3 expression and inflammasome activation in endothelial cells. HUVECs were treated with the indicated concentrations of PA (0, 100, 200, or 300 μmol/L) for 24 h, after which the supernatant was collected. ELISA was used to measure the levels of IL-1β (**A**), TNF-α (**B**), and IL-6 (**C**) release. (**D**) The protein expression of NLRP3, caspase-1, and IL-1β was analysed via Western blotting. (**E**) The bands show the quantification of the indicated proteins. Cells were pretreated with DHM for 12 h and then exposed to PA (300 μmol/L) for an additional 24 h. (**F**) ELISAs were performed to measure the levels of IL-1β. (**G**) Western blotting was used to detect the protein expression of NLRP3, caspase-1, and IL-1β. (**H**) The bands show the quantification of the indicated proteins, and the values are expressed as the fold change relative to the control group. The values are expressed as the mean ± SD ($n = 3$). $^{a}P < 0.05$ or $^{b}P < 0.01$ (versus the control group); $^{c}P < 0.05$ or $^{d}P < 0.01$ (versus the PA-treated group). DHM, dihydromyricetin; ELISA, enzyme-linked immunosorbent assay; HUVECs, human umbilical vein endothelial cells; IL-6, interleukin-6; IL-1β, interleukin-1β; NLRP3, NOD-like receptor protein 3; PA, palmitic acid; SD, standard deviation; TNFα, tumor necrosis factor α

Mitophagy hinders NF-κB from activating the endothelial NLRP3 inflammasome

In light of these findings, additional research is needed to determine whether mitophagy participates in the modulation of NLRP3 inflammasome activation in endothelial cells and to elucidate the underlying mechanisms involved. PA treatment with or without CQ significantly reduced the MTDR fluorescence intensity in endothelial cells. Pretreatment with CQ did not result in a significant change in MTDR fluorescence intensity compared to that in the PA single-treated group (Fig. 5A) [24], suggesting that mitophagy was suppressed by PA, as supported by reduced Parkin signalling, as shown in Fig. 4D. Therefore, CCCP, a potent inducer of mitophagy, was used to explore the involvement of mitophagy in the PA-induced activation of the NLRP3 inflammasome in

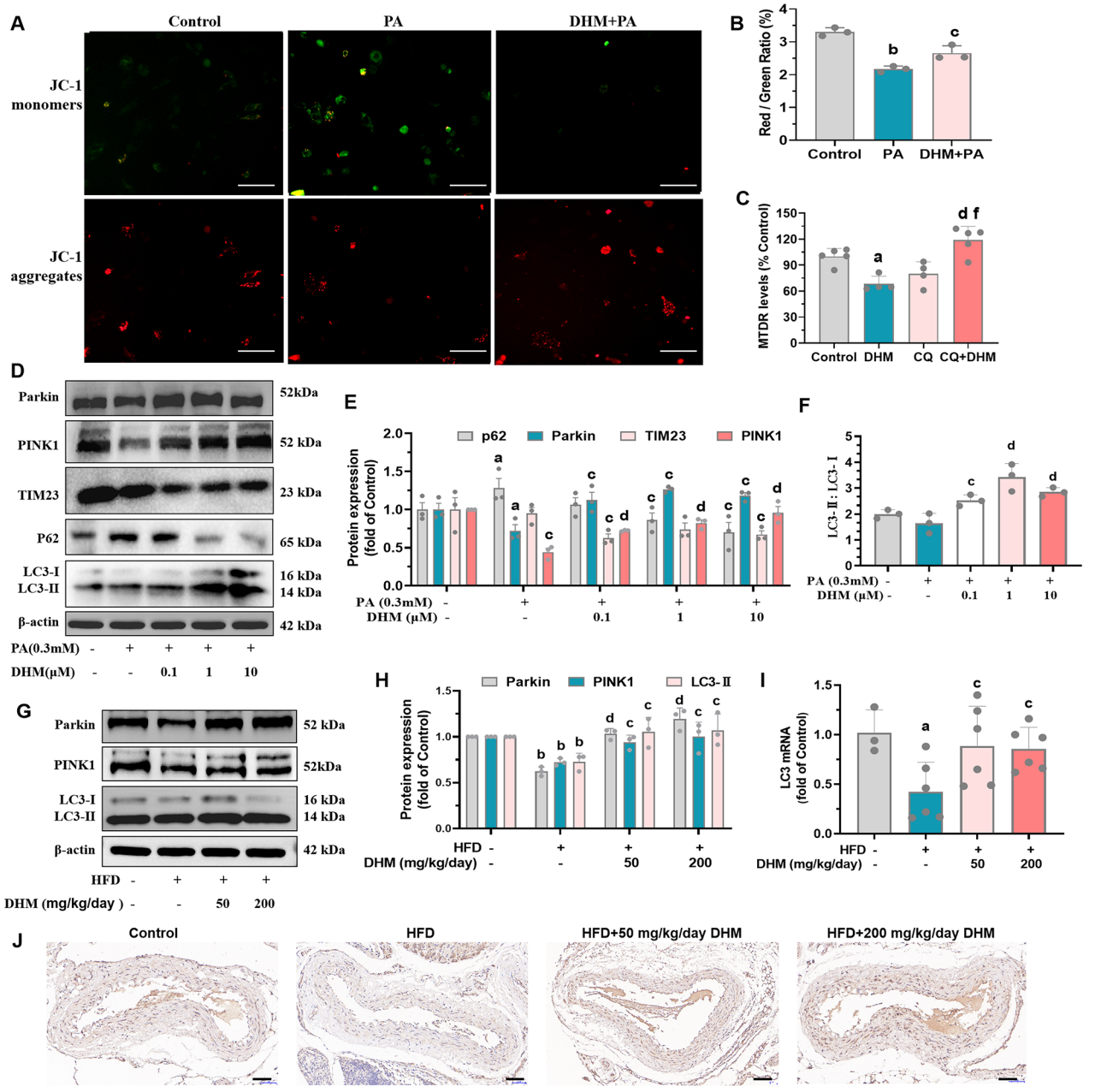

Fig. 4 DHM enhances endothelial mitophagy and mitigates mitochondrial damage. HUVECs were pretreated with DHM (1 μmol/L) for 12 h and then exposed to PA (300 μmol/L) for an additional 24 h. Subsequently, the ΔΨm was determined via JC-1 staining via a fluorescence microscope (**A**) or multi-functional microplate reader (**B**). A decrease in the ratio of red to green fluorescence indicated mitochondrial depolarization; scale bars = 50 μm. (**C**) Flow cytometry was used to analyse mitophagy via the detection of MTDR fluorescence. Cells were pretreated with DHM at various concentrations (0.1, 1, and 10 μmol/L) for 12 h, followed by PA stimulation for 24 h. (**D**) Western blotting was conducted to detect the expression of Parkin, PINK1, TIM23, p62, and LC3. (**E**) The bars show the densitometry of the bands, and the values are expressed as the fold change relative to the control group. (**F**) Analysis of the relative LC3-II:LC3 I- ratio. The values are expressed as the mean ± SD ($n = 3$). $^{a}P < 0.05$ or $^{b}P < 0.01$ (versus the control group); $^{c}P < 0.05$ or $^{d}P < 0.01$ (versus the PA-treated group); $^{f}P < 0.01$ (versus the CQ-treated group). (**G**-**H**) Western blotting was conducted to detect the expression of Parkin, PINK1 and LC3 in mouse aortas. (**I**) RT–PCR was performed to assess LC3 mRNA expression in mouse aortas. (**J**) Immunohistochemistry of Parkin in mouse aortas. Scale bars = 50 μm. The values are expressed as the mean ± SD ($n = 3$). $^{a}P < 0.05$ or $^{b}P < 0.01$, compared to the control group; $^{c}P < 0.05$ or $^{d}P < 0.01$, compared to the HFD group. CQ, chloroquine; DHM, dihydromyricetin; HFD, high-fat diet; HUVECs, human umbilical vein endothelial cells; LC3, MAP1LC3/LC3; MTDR, MitoTracker® Deep Red FM; PA, palmitic acid; Parkin, Parkin RBR E3 Ubiquitin Protein Ligase; SD, standard deviation; SQSTM1/p62, sequestosome 1; TIM23, translocase of inner mitochondrial membrane 23

vascular endothelial cells. Interestingly, the reduction in mitochondrial membrane potential and cell viability

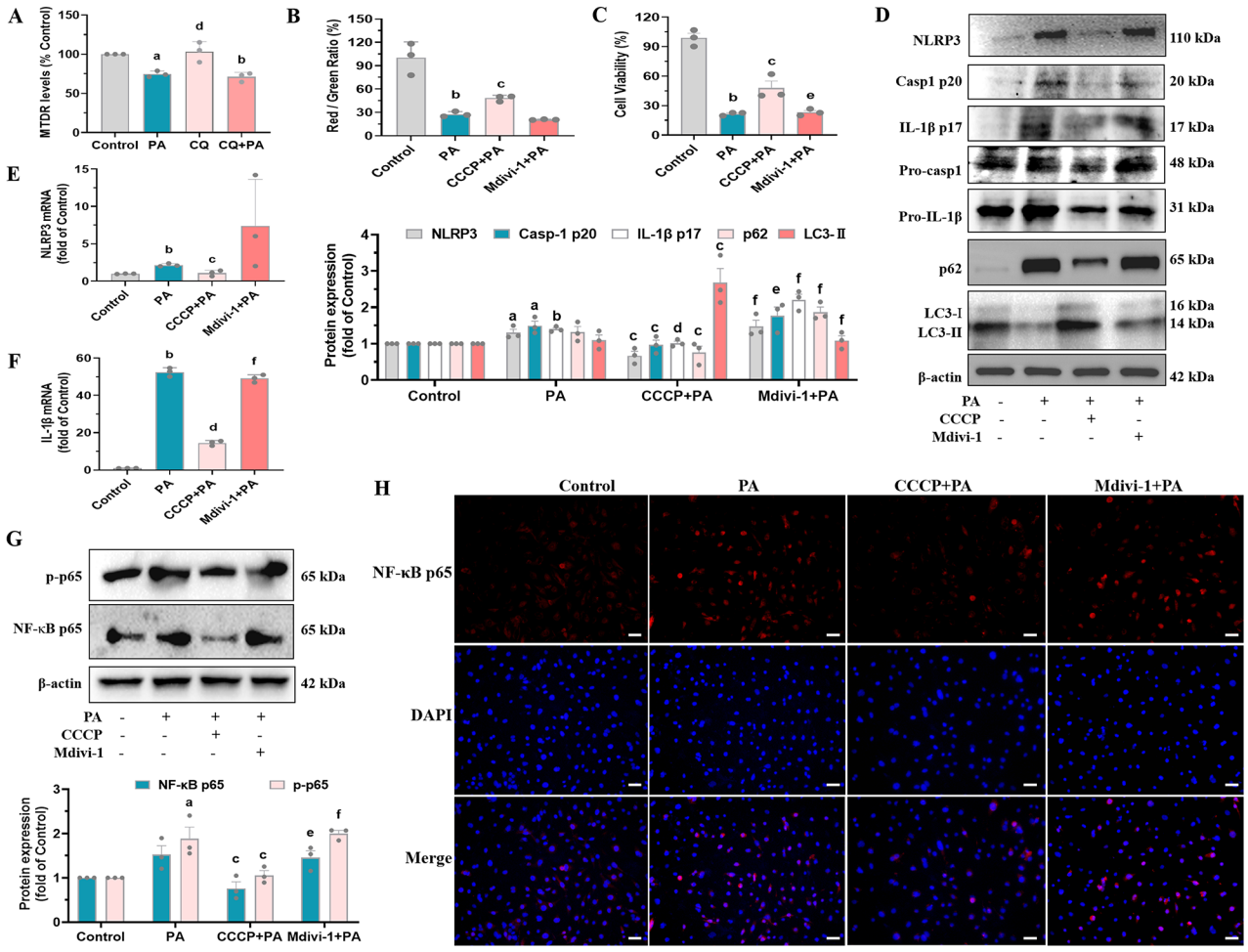

Fig. 5 Mitophagy hinders NF-κB from activating the endothelial NLRP3 inflammasome. (**A**) HUVECs were treated with 300 μmol/L PA for 24 h and co-treated with or without CQ (a lysosomal inhibitor, 25 μmol/L) for 3 h before analysis to inhibit lysosomal degradation. MTDR staining was analysed using flow cytometry. The cells were incubated with PA (300 μmol/L) for 24 h in the presence of the mitophagy inducer CCCP (10 μmol/L) or the mitophagy inhibitor Mdivi-1 (20 μmol/L). (**B**) The mitochondrial membrane potential (ΔΨm) was assessed using JC-1 staining and was examined with a multifunctional microplate reader. (**C**) Cell viability was determined using CCK-8 kits. (**D**) Western blot analysis was performed to evaluate the expression of NLRP3, Casp1 p20, IL-1β, p62, and LC3. The densitometry of the bands was quantified, and the values are expressed as the fold change relative to the control group. (E-F) RT–PCR analysis was performed to measure the mRNA expression of NLRP3 (**E**) and IL-1β (**F**). (**G**) Western blot analysis of NF-κB p65 and p-p65 expression; the bars show the densitometric analysis of the bands. (**H**) NF-κB activity was measured using an NF-κB Activation-Nuclear Translocation Assay Kit and a fluorescence microscope. Scale bar = 200 μm. The values are expressed as the mean ± SD ($n = 3$). $^{a}P < 0.05$ or $^{b}P < 0.01$ (versus the control group); $^{c}P < 0.05$ or $^{d}P < 0.01$ (versus the PA-treated group); $^{e}P < 0.05$ or $^{f}P < 0.01$ (versus the CCCP + PA group). Casp1 p20, caspase-1 p20; CCCP, carbonyl cyanide m-chlorophenyl hydrazone; CCK-8, cell counting kit; DHM, dihydromyricetin; HUVECs, human umbilical vein endothelial cells; IL-1β, interleukin-1β; LC3, MAP1LC3/LC3; Mdivi-1, mitochondrial division inhibitor 1; MTDR, MitoTracker® Deep Red FM; NF-κB, nuclear factor kappa-B; NLRP3, NOD-like receptor protein 3; PA, palmitic acid; SD, standard deviation; SQSTM1/p62, sequestosome 1

caused by PA was effectively mitigated when HUVECs were pretreated with CCCP (Fig. 5B and C). More significantly, a decrease in PA-induced NLRP3 inflammasome activation was also observed after CCCP pretreatment, as reflected by the decrease in caspase-1 cleavage and IL-1β maturation (Fig. 5D). Collectively, these data demonstrate that increasing mitophagy inhibits NLRP3 inflammasome activation in vascular endothelial cells.

The cellular NLRP3 level is a critical determinant of the assembly and activation of the NLRP3 inflammasome [32]. The above results illustrated that mitophagy inhibits NLRP3 protein expression. Additionally, we found that the mitophagy inducer CCCP significantly reduced the mRNA expression of NLRP3 and IL-1β (Fig. 5E and F), indicating that mitophagy selectively regulates NLRP3 expression at both the protein and mRNA levels. These findings prompted us to investigate the potential effects of mitophagy on the expression and activation of NF-κB, a key transcription factor that governs NLRP3 and IL-1β transcription [33]. As anticipated, increasing mitophagy via CCCP significantly suppressed PA-induced expression and phosphorylation of NF-κB p65 (Fig. 5G)

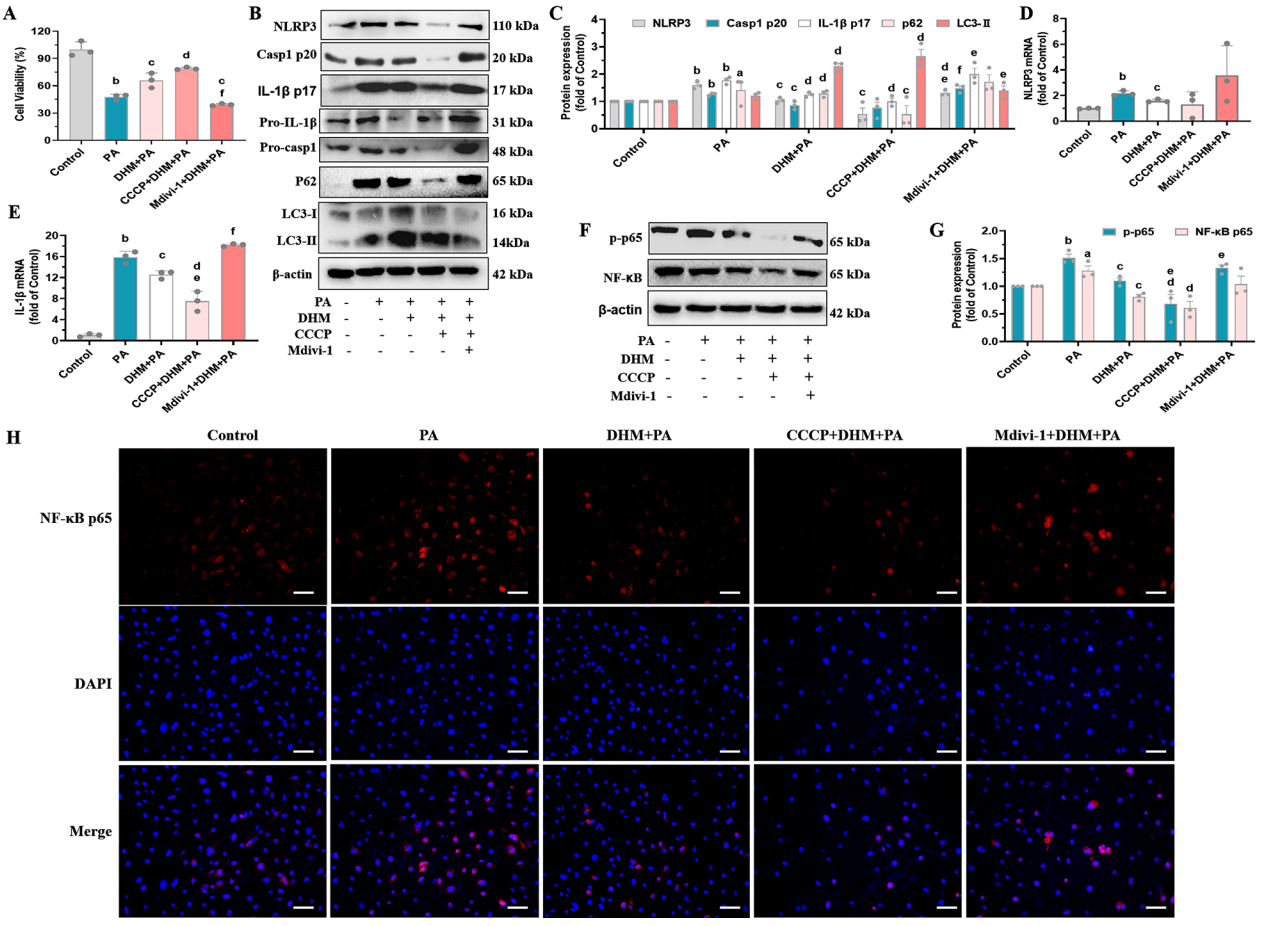

Fig. 6 DHM impedes endothelial NLRP3 inflammasome activation by promoting mitophagy. HUVECs were pretreated with DHM (1 μmol/L) for 12 h in the presence of the mitophagy inducer CCCP (10 μmol/L) or the mitophagy inhibitor Mdivi-1 (20 μmol/L) and then stimulated with PA (300 μmol/L) for another 24 h. (**A**) Cell viability was determined using CCK-8 kits. (**B**) Western blot analysis of NLRP3, caspase-1, IL-1β, p62 and LC3 expression. (**C**) The bars show the densitometry of the bands. (D-E) RT–PCR analysis of NLRP3 (**D**) and IL-1β (**E**) mRNA expression. (**F**-**G**) Western blot analysis of NF-κB p65 and p-p65 expression; the bars show the densitometry of the bands. (**H**) NF-κB activity was measured using an NF-κB Activation-Nuclear Translocation Assay Kit and a fluorescence microscope. Scale bars = 200 μm. The values are expressed as the mean ± SD ($n = 3$). $^{a}P < 0.05$ or $^{b}P < 0.01$, versus the control group; $^{c}P < 0.05$ or $^{d}P < 0.01$, versus the PA-treated group; $^{e}P < 0.05$ or $^{f}P < 0.01$, versus the DHM + PA group. Casp1 p20, caspase-1 p20; CCCP, carbonyl cyanide m-chlorophenyl hydrazone; CCK-8, cell counting kit; DHM, dihydromyricetin; HUVECs, human umbilical vein endothelial cells; IL-1β, interleukin-1β; LC3, MAP1LC3/LC3; Mdivi-1, mitochondrial division inhibitor 1; MTDR, MitoTracker® Deep Red FM; NF-κB, nuclear factor kappa-B; NLRP3, NOD-like receptor protein 3; PA, palmitic acid; SD, standard deviation; SQSTM1/p62, sequestosome 1

and reduced the nuclear translocation of NF-κB p65 (Fig. 5H). Collectively, these data suggest that increasing mitophagy can hinder PA-mediated activation of NF-κB p65, thereby reducing NLRP3 expression and inflammasome activation in endothelial cells.

Further analysis revealed that pretreatment with Mdivi-1, a mitophagy inhibitor, did not significantly alter the activation of NF-κB or NLRP3 compared to PA treatment alone (Fig. 5). This could be attributed to the considerable inhibition of endothelial mitophagy already exerted by PA and the robust activating impact of PA on the NLRP3 inflammasome. Consequently, the additional suppression of mitophagy by Mdivi-1 did not intensify the PA-induced activation of the NLRP3 inflammasome.

DHM impedes endothelial NLRP3 inflammasome activation by promoting mitophagy

As mentioned above, DHM suppressed NLRP3 inflammasome activation in vascular endothelial cells [3]. Moreover, based on the results presented in Fig. 4, which demonstrated that DHM promoted mitophagy and maintained mitochondrial homeostasis, we hypothesized that mitophagy could be a critical factor through which DHM inhibits NLRP3 inflammasome activation. To confirm this, endothelial cells were pretreated with DHM in the presence of the mitophagy inducer CCCP or the mitophagy inhibitor Mdivi-1 and then stimulated with PA for another 24 h. DHM significantly abrogated the PA-induced reduction in cell viability, but this protective effect was diminished by the mitophagy inhibitor

Mdivi-1 (Fig. 6A). Moreover, we found that the downregulation of NLRP3, Casp1 p20, and IL-1β p17 protein expression in the DHM group, compared to the PA group, was further intensified by the mitophagy agonist CCCP, while this change was partially reversed by the mitophagy inhibitor Mdivi-1 (Fig. 6B and C). These findings indicate that mitophagy likely plays a pivotal role in DHM-mediated blockade of endothelial NLRP3 inflammasome activation.

As shown in Fig. 6, DHM pretreatment significantly reduced the mRNA expression of NLRP3 and IL-1β (Fig. 6D and E), indicating that DHM may also regulate the priming process (signal 1) of NLRP3 inflammasome activation. These findings encouraged us to investigate the potential effects of DHM on the activation of NF-κB, a key transcription factor that governs NLRP3 and IL-1β [33]. As anticipated, DHM pretreatment markedly inhibited the PA-induced expression and phosphorylation of NF-κB p65 (Fig. 6F and G) and simultaneously inhibited NF-κB activation and nuclear translocation (Fig. 6H). Furthermore, the inhibition of NF-κB p65 activation by DHM was further enhanced by CCCP pretreatment, while this effect was partially abrogated when mitophagy was inhibited by the mitophagy inhibitor Mdivi-1 (Fig. 6F and H). Collectively, these results suggest that DHM inhibits the activation of NF-κB p65 by promoting mitophagy, thereby reducing endothelial NLRP3 inflammasome activation in response to PA stimuli.

Discussion

The present study demonstrated that DHM emerges as a potential mitophagy promoter, and DHM administration reduces atherogenesis by inhibiting NLRP3 inflammasome activation and diminishing inflammation. In vascular endothelial cells, excessive PA (a saturated fatty acid) engenders mitochondrial damage, activating NF-κB and the subsequent NLRP3 inflammasome. However, either promoting mitophagy or administering DHM can attenuate these effects. Notably, DHM inhibited PA-stimulated NF-κB activation and nuclear translocation by facilitating mitophagy, thereby curtailing the expression of NLRP3 and IL-1β, and ultimately blocking NLRP3 inflammasome activation and IL-1β secretion. This study highlights novel mechanisms and potential therapeutic strategies for preventing and treating atherosclerosis.

Atherosclerosis is a chronic disease characterized by lipid deposition and inflammation beneath the vessel intima [34]. This study showed that a HFD leads to dyslipidaemia and vascular inflammation in ApoE$^{-/-}$ mice, accelerating the formation and development of atherosclerosis. According to the "response-to-injury" hypothesis proposed by Ross and Glomset, vascular endothelial dysfunction resulting from various cardiovascular risk factors is considered the underlying cause of atherosclerotic lesions [27, 35, 36]. Therefore, reducing endothelial dysfunction has become a key priority in atherosclerosis management. Epidemiological evidence suggests that flavonoids, which occur ubiquitously in foodstuffs of plant origin, possess diverse bioactivities, such as lipid-lowering, anti-inflammatory, and antioxidant effects, and have the potential to reduce the risk of chronic diseases such as CVD and diabetes [37, 38]. Previous studies have demonstrated that DHM, a naturally occurring flavonoid, can attenuate inflammatory damage in vascular endothelial cells and might be a potential therapeutic adjuvant for treating atherosclerosis [3, 10, 17]. Therefore, this study administered DHM to mice fed a HFD for 14 weeks and observed a substantial decrease in the formation of atherosclerotic plaques, along with reduced serum levels of TC, TG, and LDL-C. Concurrently, there was an observable increase in the concentration of HDL-C. Moreover, DHM intervention markedly improved the serum inflammatory profile, as determined by the levels of IL-1β, IL-18, IL-6, and TNF-α. This alteration aligns with previous studies [10, 17]. Notably, this study used lower concentrations of DHM (50 mg/kg and 200 mg/kg) and revealed that even at a lower concentration (50 mg/kg), DHM notably attenuated inflammation and atherosclerotic lesion formation. In addition, 50 mg/kg DHM exhibited inhibitory effects on NLRP3 inflammasome activation and vascular inflammation akin to those of 200 mg/kg DHM, and these findings are intriguing and align with the findings of previous studies. For instance, a study revealed no significant differences in blood lipid profiles or inflammation levels between LDLr(-/-) mice fed a HFD treated with 250 mg/kg DHM or 500 mg/kg DHM [10]. Similarly, another study investigating the effects of DHM on hepatic insulin resistance induced by a HFD did not reveal significant disparities in lipid homeostasis or blood glucose levels across DHM (100, 200, and 400 mg/kg) treatment groups [16]. Additionally, a large cross-sectional investigation established a nonlinear, J-shaped relationship between flavonoid intake and the risk of coronary artery disease (nonlinear test $P<0.05$) [39]. Consequently, it is speculated that the effects of DHM do not conform to a simple linear dose-dependent model but exhibit intricate nonlinear associations, which may be attributed to the metabolic pathways of DHM within the organism, the saturation of its target sites, and the modulation of endogenous bioactive compounds.

The NLRP3 inflammasome, a key receptor/sensor involved in innate immunity, is responsible for the progression and instability of atherosclerosis [40]. In humans and animals, hypernomic NLRP3 inflammasome activation has been implicated in arterial plaque formation, while genetic knockout or inhibition of NLRP3 could improve endothelial cell function and reduce the

atherosclerotic plaque area [2, 26], highlighting NLRP3 as an important target for combating atherosclerosis [26, 41]. Animal foods, such as red meat (beef, lamb, pork, etc.), offal, and some dairy products, are rich in saturated fatty acids (e.g., PA), and excessive intake of saturated fatty acids can trigger an increase in plasma lipid levels, especially LDL-C levels, thereby increasing the risk of atherosclerosis. Here, both endothelial cells treated with PA and atherosclerosis model mice fed a high-fat diet exhibited significantly increased NLRP3 inflammasome activation and elevated IL-1β release. IL-1β is a major proinflammatory factor in the early stages of arterial plaque formation and contributes to atherosclerosis pathogenesis [42]. However, with DHM intervention, the ability of PA to induce NLRP3 inflammasome activation and IL-1β release was significantly reduced. As activation of the NLRP3 inflammasome requires two signals—a priming signal and an activation signal [4]—this study further demonstrated that DHM blocks NLRP3 expression at both the protein and mRNA levels. This likely indicates that DHM inhibits the priming signal, which depends on NF-κB. Previous evidence suggests that DHM modulates NF-κB signalling by directly interacting with IκB kinase (IKK), thus reducing the phosphorylation of IKK and ameliorating inflammation [43]. DHM can increase SIRT3 (Sirtuin 3) signalling to deactivate the NF-κB and NLRP3 pathways [44–46].

Mitochondrial damage has been implicated in the assembly and activation of the NLRP3 inflammasome [7, 30, 47]. Studies generally suggest that dysfunctional mitochondria release mitochondrial ROS or mitochondrial DNA, which is indispensable for NLRP3 inflammasome activation in response to diverse inflammasome-activating stimuli [8, 30, 48]. However, few studies have reported that damaged mitochondria also engage in priming signals for NLRP3 inflammasome activation [33]. Notably, this study showed that the excessive presence of PA impaired mitochondrial function and activated the transcription factor NF-κB, which is essential for NLRP3 transcription. Moreover, increasing evidence suggests that mitophagy, a selective form of autophagy, plays a crucial role in removing damaged mitochondria and maintaining cellular homeostasis in response to various stressors, thereby inhibiting NLRP3 inflammasome activation [49–51]. Consistent with these findings, this study demonstrated that the mitophagy agonist CCCP significantly ameliorated mitochondrial dysfunction and suppressed NLRP3 inflammasome activation in response to PA stimuli. In contrast, the administration of the mitophagy inhibitor Mdivi-1 or the knockout of the LC3 gene, a key autophagic protein, results in the buildup of impaired mitochondria and excessive activation of the NLRP3 inflammasome [50]. Surprisingly, similar to CCCP, DHM facilitated mitophagy and restored endothelial mitochondrial homeostasis under PA-stimulated conditions, thereby inhibiting NLRP3 inflammasome activation; however, once the cells were incubated with the mitophagy inhibitor Mdivi-1, DHM no longer exerted its effects. These findings indicate that mitophagy is essential for DHM-mediated inhibition of endothelial NLRP3 inflammasome activation under high-fat conditions. Further investigations are warranted to elucidate the specific mechanisms through which mitophagy regulates high-fat diet-induced NLRP3 inflammasome activation within the aortic endothelium.

The protein expression of NLRP3, regarded as a rate-limiting step for NLRP3 inflammasome activation [32], is controlled principally by the transcription factor NF-κB, which initiates NLRP3 transcription. Numerous studies have demonstrated that saturated fatty acids (e.g., palmitic acid) activate NF-κB and increase the secretion of inflammatory cytokines [52], which is consistent with our findings. Although evidence has shown associations between these inflammatory cytokines and mitochondrial dysfunction in several cell types [53, 54], studies linking the classical NF-κB pathway to mitochondrial dysfunction in the context of endothelial cellular fuel overloading (such as excessive saturated fatty acids) are sparse. As anticipated, in this study, treatment of endothelial cells with high PA concentrations contributed significantly to disruptions in mitochondrial homeostasis. This, in turn, activated NF-κB by phosphorylating p65 and increasing nuclear translocation, subsequently upregulating the expression of NLRP3 and pro-IL-1β. However, following the induction of mitophagy through CCCP or DHM pretreatment, mitochondrial dysfunction was ameliorated, resulting in reduced activation of NF-κB p65. These findings suggested that endothelial NF-κB activity is triggered by PA-induced mitochondrial dysfunction. These findings differ from those of a previous study [55], which demonstrated that NF-κB signalling induces mitochondrial dysfunction in skeletal muscle due to nutrient overload. Moreover, under DHM pretreatment conditions, the mitophagy inducer CCCP further blocked PA-induced NF-κB activity and subsequent NLRP3 expression and inflammasome activation. Conversely, when mitophagy was inhibited by the mitophagy inhibitor Mdivi-1, the inhibitory effect of DHM on PA-stimulated NF-κB activity was significantly attenuated. These results demonstrated that DHM interferes with NF-κB activity and suppresses NLRP3 expression and inflammasome activation by enhancing mitophagy.

Strengths and limitations

The strength of this study is that it combines an in vivo animal model of atherosclerosis and an in vitro model of endothelial cell injury. This dual approach provides insights into the precise molecular mechanisms through

which DHM attenuates atherosclerosis, thereby increasing the credibility of the findings and providing robust evidence to support population-based intervention trials. This study also identified potential strategies to combat atherosclerosis and provided new insights into the potential mechanisms by which mitophagy regulates NLRP3 inflammasome activation. Although this study provides evidence that DHM induces mitophagy, the specific mechanism involved has not been elucidated. Therefore, the specific molecular targets underlying the modulation of mitophagy by DHM will be the focus of future research. Future efforts will be directed towards a comprehensive analysis of these targets to reveal the exact molecular mechanism through which DHM exerts its effects.

Conclusions

In conclusion, this study suggested that DHM can facilitate mitophagy to reduce endothelial NLRP3 inflammasome activation and thereby effectively alleviate atherosclerosis. Exposure to PA leads to endothelial mitochondrial damage, which triggers the activation and nuclear translocation of NF-κB p65. This, in turn, increases cellular NLRP3 levels and inflammasome activation. Surprisingly, upregulating mitophagy or administering DHM can mitigate this process. Importantly, the inhibitory effect of DHM on NLRP3 inflammasome activation is partially dependent on its ability to induce mitophagy. Although additional mechanisms by which DHM inhibits the NLRP3 inflammasome cannot be entirely dismissed, molecular investigations conducted herein support the proposal that DHM promotes endothelial mitophagy to maintain normal mitochondrial functionality, thereby preventing NF-κB from activating the NLRP3 inflammasome and reducing the subsequent release of IL-1β. Consequently, DHM can function as a compelling promoter of mitophagy and has potential as a therapeutic adjunct for treating atherosclerosis and other inflammatory diseases marked by abnormal NLRP3 activity.

Abbreviations

ANOVA	Analysis of Variance
ApoE$^{-/-}$	Apolipoprotein E-deficient
ATCC	American Type Culture Collection
Casp1 p20	Caspase-1 p20
CCCP	Carbonyl Cyanide m-Chlorophenyl hydrazone
CCK-8	Cell Counting Kit-8
CQ	Chloroquine
DHM	Dihydromyricetin
DMSO	Dimethyl Sulfoxide
ECGS	Endothelial Cell Growth Supplement
ECM	Endothelial Cell Medium
ELISA	Enzyme-Linked Immunosorbent Assay
FBS	Fetal Bovine Serum
HDL-C	High-density lipoprotein cholesterol
HFD	High-Fat Diet
HUVECs	Human Umbilical Vein Endothelial Cells
IL-6	Interleukin-6
IL-18	Interleukin-18
IL-1β	Interleukin-1β
IKK	IκB kinase
LC3	MAP1LC3/LC3
LDL-C	Low-density lipoprotein cholesterol
Mdivi-1	Mitochondrial division inhibitor 1
MTDR	MitoTracker® Deep Red FM
NF-κB	Nuclear factor kappa-B
NLRP3	NOD-like receptor protein 3
PA	Palmitic acid
Parkin	Parkin RBR E3 Ubiquitin Protein Ligase
PINK1	PTEN induced putative kinase 1
p-p65	Phospho-NF-κB p65
Pro-casp1	Pro-caspase-1
SD	Standard deviation
SIRT3	Sirtuin 3
SQSTM1/p62	Sequestosome 1
TC	Total cholesterol
TG	Triglycerides
TIM23	Translocase of inner mitochondrial membrane 23
TNF-α	Tumor necrosis factor-α
ΔΨm	Mitochondrial membrane potential

Supplementary Information

The online version contains supplementary material available at https://doi.org/10.1186/s12944-024-02263-1.

Supplementary Material 1

Author contributions

HQ conceived and designed the study, performed the experiments, prepared the figures and/or tables, authored or reviewed drafts of the article. LCY, SYF, RL, and SH performed the experiments, prepared the figures and/or tables. ZT, YL, CTJ, and MXY analysed the data, revised the article critically for important content. LYF conceived and designed the study, authored or reviewed drafts of the article. All authors approved the final draft.

Funding

This study was supported by grants from the National Natural Science Foundation of China (81803229) and the Natural Science Foundation Project of Chongqing, China (cstc2020jcyj-msxmX0105).

Data availability

No datasets were generated or analysed during the current study.

Declarations

Ethical approval

The study was approved by the Laboratory Animal Welfare and Ethics Committee of the Third Military Medical University (Chongqing, China).

Consent for publication

Not applicable.

Competing interests

The authors declare no competing interests.

Author details

[1]Department of Epidemiology, Institute of Military Preventive Medicine, Army Medical University (Third Military Medical University), Chongqing 400038, P. R. China
[2]Research Center for Nutrition and Food Safety, Institute of Military Preventive Medicine, Army Medical University (Third Military Medical University), Chongqing 400038, P. R. China

Received: 10 July 2024 / Accepted: 18 August 2024
Published online: 03 September 2024

References

1. Zhuang T, Liu J, Chen X, Zhang L, Pi J, Sun H, Li L, Bauer R, Wang H, Yu Z, et al. Endothelial Foxp1 suppresses atherosclerosis via modulation of Nlrp3 inflammasome activation. CIRC RES. 2019;125(6):590–605.
2. Zhang Y, Li X, Pitzer AL, Chen Y, Wang L, Li PL. Coronary endothelial dysfunction induced by nucleotide oligomerization domain-like receptor protein with pyrin domain containing 3 inflammasome activation during hypercholesterolemia: beyond inflammation. Antioxid Redox Signal. 2015;22(13):1084–96.
3. Hu Q, Zhang T, Yi L, Zhou X, Mi M. Dihydromyricetin inhibits NLRP3 inflammasome-dependent pyroptosis by activating the Nrf2 signaling pathway in vascular endothelial cells. BioFactors. 2018;44(2):123–36.
4. Swanson KV, Deng M, Ting JP. The NLRP3 inflammasome: molecular activation and regulation to therapeutics. NAT REV IMMUNOL. 2019;19(8):477–89.
5. Lamkanfi M, Dixit VM. Mechanisms and functions of inflammasomes. Cell. 2014;157(5):1013–22.
6. Strowig T, Henao-Mejia J, Elinav E, Flavell R. Inflammasomes in health and disease. Nature. 2012;481(7381):278–86.
7. Rovira-Llopis S, Apostolova N, Banuls C, Muntane J, Rocha M, Victor VM. Mitochondria, the NLRP3 Inflammasome, and sirtuins in type 2 diabetes: new therapeutic targets. Antioxid Redox Signal. 2018;29(8):749–91.
8. Zhong Z, Liang S, Sanchez-Lopez E, He F, Shalapour S, Lin XJ, Wong J, Ding S, Seki E, Schnabl B, et al. New mitochondrial DNA synthesis enables NLRP3 inflammasome activation. Nature. 2018;560(7717):198–203.
9. Teresak P, Lapao A, Subic N, Boya P, Elazar Z, Simonsen A. Regulation of PRKN-independent mitophagy. AUTOPHAGY. 2022;18(1):24–39.
10. Liu TT, Zeng Y, Tang K, Chen X, Zhang W, Xu XL. Dihydromyricetin ameliorates atherosclerosis in LDL receptor deficient mice. ATHEROSCLEROSIS. 2017;262:39–50.
11. Liang X, Zhang T, Shi L, Kang C, Wan J, Zhou Y, Zhu J, Mi M. Ampelopsin protects endothelial cells from hyperglycemia-induced oxidative damage by inducing autophagy via the AMPK signaling pathway. BioFactors. 2015;41(6):463–75.
12. Shi L, Zhang T, Liang X, Hu Q, Huang J, Zhou Y, Chen M, Zhang Q, Zhu J, Mi M. Dihydromyricetin improves skeletal muscle insulin resistance by inducing autophagy via the AMPK signaling pathway. MOL CELL ENDOCRINOL. 2015;409:92–102.
13. Wei Y, Lan B, Zheng T, Yang L, Zhang X, Cheng L, Tuerhongjiang G, Yuan Z, Wu Y. GSDME-mediated pyroptosis promotes the progression and associated inflammation of atherosclerosis. NAT COMMUN. 2023;14(1):929.
14. Karunakaran D, Nguyen MA, Geoffrion M, Vreeken D, Lister Z, Cheng HS, Otte N, Essebier P, Wyatt H, Kandiah JW, et al. RIPK1 expression associates with inflammation in early atherosclerosis in humans and can be therapeutically silenced to reduce NF-kappaB activation and atherogenesis in mice. Circulation. 2021;143(2):163–77.
15. He L, Chen Q, Wang L, Pu Y, Huang J, Cheng CK, Luo JY, Kang L, Lin X, Xiang L, et al. Activation of Nrf2 inhibits atherosclerosis in ApoE(-/-) mice through suppressing endothelial cell inflammation and lipid peroxidation. REDOX BIOL. 2024;74:103229.
16. Le L, Jiang B, Wan W, Zhai W, Xu L, Hu K, Xiao P. Metabolomics reveals the protective of Dihydromyricetin on glucose homeostasis by enhancing insulin sensitivity. Sci Rep. 2016;6:36184.
17. Yang D, Yang Z, Chen L, Kuang D, Zou Y, Li J, Deng X, Luo S, Luo J, He J, et al. Dihydromyricetin increases endothelial nitric oxide production and inhibits atherosclerosis through microRNA-21 in apolipoprotein E-deficient mice. J CELL MOL MED. 2020;24(10):5911–25.
18. Zeng X, Yang J, Hu O, Huang J, Ran L, Chen M, Zhang Y, Zhou X, Zhu J, Zhang Q, et al. Dihydromyricetin ameliorates nonalcoholic fatty liver disease by improving mitochondrial respiratory capacity and Redox Homeostasis through Modulation of SIRT3 Signaling. Antioxid Redox Signal. 2019;30(2):163–83.
19. Karunakaran D, Geoffrion M, Wei L, Gan W, Richards L, Shangari P, DeKemp EM, Beanlands RA, Perisic L, Maegdefessel L, et al. Targeting macrophage necroptosis for therapeutic and diagnostic interventions in atherosclerosis. SCI ADV. 2016;2(7):e1600224.
20. Zhang T, Hu Q, Shi L, Qin L, Zhang Q, Mi M. Equol attenuates atherosclerosis in apolipoprotein E-Deficient mice by inhibiting endoplasmic reticulum stress via activation of Nrf2 in endothelial cells. PLoS ONE. 2016;11(12):e167020.
21. Paigen B, Morrow A, Holmes PA, Mitchell D, Williams RA. Quantitative assessment of atherosclerotic lesions in mice. ATHEROSCLEROSIS. 1987;68(3):231–40.
22. Xu F, Guo M, Huang W, Feng L, Zhu J, Luo K, Gao J, Zheng B, Kong LD, Pang T, et al. Annexin A5 regulates hepatic macrophage polarization via directly targeting PKM2 and ameliorates NASH. REDOX BIOL. 2020;36:101634.
23. Zhang Z, Yan J, Bowman AB, Bryan MR, Singh R, Aschner M. Dysregulation of TFEB contributes to manganese-induced autophagic failure and mitochondrial dysfunction in astrocytes. *AUTOPHAGY* 2020, 16(8):1506–1523.
24. Mauro-Lizcano M, Esteban-Martínez L, Seco E, Serrano-Puebla A, Garcia-Ledo L, Figueiredo-Pereira C, Vieira HLA, Boya P. New method to assess mitophagy flux by flow cytometry. AUTOPHAGY. 2015;11(5):833–43.
25. Fu ZJ, Wang ZY, Xu L, Chen XH, Li XX, Liao WT, Ma HK, Jiang MD, Xu TT, Xu J, et al. HIF-1alpha-BNIP3-mediated mitophagy in tubular cells protects against renal ischemia/reperfusion injury. REDOX BIOL. 2020;36:101671.
26. Duewell P, Kono H, Rayner KJ, Sirois CM, Vladimer G, Bauernfeind FG, Abela GS, Franchi L, Nunez G, Schnurr M, et al. NLRP3 inflammasomes are required for atherogenesis and activated by cholesterol crystals. Nature. 2010;464(7293):1357–61.
27. Gimbrone MJ, Garcia-Cardena G. Endothelial cell dysfunction and the pathobiology of atherosclerosis. CIRC RES. 2016;118(4):620–36.
28. Medina-Leyte DJ, Zepeda-Garcia O, Dominguez-Perez M, Gonzalez-Garrido A, Villarreal-Molina T, Jacobo-Albavera L. Endothelial dysfunction, inflammation and coronary artery disease: potential biomarkers and promising therapeutical approaches. INT J MOL SCI 2021, 22(8).
29. Mishra SR, Mahapatra KK, Behera BP, Patra S, Bhol CS, Panigrahi DP, Praharaj PP, Singh A, Patil S, Dhiman R, et al. Mitochondrial dysfunction as a driver of NLRP3 inflammasome activation and its modulation through mitophagy for potential therapeutics. Int J Biochem Cell Biol. 2021;136:106013.
30. Zhou R, Yazdi AS, Menu P, Tschopp J. A role for mitochondria in NLRP3 inflammasome activation. Nature. 2011;469(7329):221–5.
31. Ma S, Chen J, Feng J, Zhang R, Fan M, Han D, Li X, Li C, Ren J, Wang Y et al. Melatonin Ameliorates the Progression of Atherosclerosis via Mitophagy Activation and NLRP3 Inflammasome Inhibition. *OXID MED CELL LONGEV* 2018, 2018:9286458.
32. Song H, Zhao C, Yu Z, Li Q, Yan R, Qin Y, Jia M, Zhao W. UAF1 deubiquitinase complexes facilitate NLRP3 inflammasome activation by promoting NLRP3 expression. NAT COMMUN. 2020;11(1):6042.
33. Zhong Z, Umemura A, Sanchez-Lopez E, Liang S, Shalapour S, Wong J, He F, Boassa D, Perkins G, Ali SR, et al. NF-kappaB restricts Inflammasome Activation via Elimination of Damaged Mitochondria. Cell. 2016;164(5):896–910.
34. Malekmohammad K, Bezsonov EE, Rafieian-Kopaei M. Role of lipid Accumulation and inflammation in atherosclerosis: focus on Molecular and Cellular mechanisms. Front Cardiovasc Med. 2021;8:707529.
35. Botts SR, Fish JE, Howe KL. Dysfunctional vascular endothelium as a driver of atherosclerosis: emerging insights into pathogenesis and treatment. FRONT PHARMACOL. 2021;12:787541.
36. Ross R, Glomset JA. The pathogenesis of atherosclerosis (first of two parts). N Engl J Med. 1976;295(7):369–77.
37. Maleki SJ, Crespo JF, Cabanillas B. Anti-inflammatory effects of flavonoids. FOOD CHEM. 2019;299:125124.
38. Kozlowska A, Szostak-Wegierek D. Flavonoids–food sources and health benefits. Rocz Panstw Zakl Hig. 2014;65(2):79–85.
39. Guo Q, Wang L, Qu Q, Cheang I, Li X, Pang H, Liao S. Association of flavonoid intake with coronary artery disease risk in the older population based on the National Health and Nutrition Examination Survey. Environ Sci Pollut Res Int. 2024;31(3):3815–27.
40. Wang S, Lei T, Zhang K, Zhao W, Fang L, Lai B, Han J, Xiao L, Wang N. Xenobiotic pregnane X receptor (PXR) regulates innate immunity via activation of NLRP3 inflammasome in vascular endothelial cells. J BIOL CHEM. 2014;289(43):30075–81.
41. Fuster JJ, MacLauchlan S, Zuriaga MA, Polackal MN, Ostriker AC, Chakraborty R, Wu CL, Sano S, Muralidharan S, Rius C, et al. Clonal hematopoiesis associated with TET2 deficiency accelerates atherosclerosis development in mice. Science. 2017;355(6327):842–7.
42. Warnatsch A, Ioannou M, Wang Q, Papayannopoulos V. Inflammation. Neutrophil extracellular traps license macrophages for cytokine production in atherosclerosis. Science. 2015;349(6245):316–20.
43. Sun Y, Liu S, Yang S, Chen C, Yang Y, Lin M, Liu C, Wang W, Zhou X, Ai Q, et al. Mechanism of Dihydromyricetin on Inflammatory diseases. FRONT PHARMACOL. 2021;12:794563.
44. Sun CC, Li Y, Yin ZP, Zhang QF. Physicochemical properties of dihydromyricetin and the effects of ascorbic acid on its stability and bioavailability. J Sci Food Agric. 2021;101(9):3862–9.

45. Shen T, Wu Y, Wang X, Wang Z, Li E, Zhou C, Yue C, Jiang Z, Wei G, Lian J, et al. Activating SIRT3 in peritoneal mesothelial cells alleviates postsurgical peritoneal adhesion formation by decreasing oxidative stress and inhibiting the NLRP3 inflammasome. EXP MOL MED. 2022;54(9):1486–501.
46. Yu H, Liu Q, Chen G, Huang L, Luo M, Lv D, Luo S. SIRT3-AMPK signaling pathway as a protective target in endothelial dysfunction of early sepsis. INT IMMUNOPHARMACOL. 2022;106:108600.
47. Gurung P, Lukens JR, Kanneganti TD. Mitochondria: diversity in the regulation of the NLRP3 inflammasome. TRENDS MOL MED. 2015;21(3):193–201.
48. Murphy MP. Newly made mitochondrial DNA drives inflammation. Nature. 2018;560(7717):176–7.
49. Nakahira K, Haspel JA, Rathinam VA, Lee SJ, Dolinay T, Lam HC, Englert JA, Rabinovitch M, Cernadas M, Kim HP, et al. Autophagy proteins regulate innate immune responses by inhibiting the release of mitochondrial DNA mediated by the NALP3 inflammasome. NAT IMMUNOL. 2011;12(3):222–30.
50. Lupfer C, Thomas PG, Anand PK, Vogel P, Milasta S, Martinez J, Huang G, Green M, Kundu M, Chi H, et al. Receptor interacting protein kinase 2-mediated mitophagy regulates inflammasome activation during virus infection. NAT IMMUNOL. 2013;14(5):480–8.
51. Liu K, Zhou X, Fang L, Dong J, Cui L, Li J, Meng X, Zhu G, Li J, Wang H. PINK1/parkin-mediated mitophagy alleviates Staphylococcus aureus-induced NLRP3 inflammasome and NF-kappaB pathway activation in bovine mammary epithelial cells. INT IMMUNOPHARMACOL. 2022;112:109200.
52. Haversen L, Danielsson KN, Fogelstrand L, Wiklund O. Induction of proinflammatory cytokines by long-chain saturated fatty acids in human macrophages. ATHEROSCLEROSIS. 2009;202(2):382–93.
53. Ji C, Chen X, Gao C, Jiao L, Wang J, Xu G, Fu H, Guo X, Zhao Y. IL-6 induces lipolysis and mitochondrial dysfunction, but does not affect insulin-mediated glucose transport in 3T3-L1 adipocytes. J BIOENERG BIOMEMBR. 2011;43(4):367–75.
54. Youle RJ. Mitochondria-Striking a balance between host and endosymbiont. *SCIENCE* 2019, 365(6454).
55. Nisr RB, Shah DS, Ganley IG, Hundal HS. Proinflammatory NFkB signalling promotes mitochondrial dysfunction in skeletal muscle in response to cellular fuel overloading. CELL MOL LIFE SCI. 2019;76(24):4887–904.

Publisher's note